

**Cover Story**

## Optimizing Pb-Free SMT Process Parameters

A Taguchi approach reveals the most important process steps and best settings for screen-printing and reflow, as well as the best combination of paste and board finishes for lead-free soldering.

**Antonio Buonomo, Alessandro Lo Schiavo and Fabrizio Rotulo**

Many investigations have focused on a suitable replacement of the SnPb eutectic solder alloy. As there is no drop-in replacement for SnPb solder capable of maintaining the necessary combination of mechanical properties, cost manufacturability, availability and reliability, a majority of the industries have decided to replace it with SnAgCu alloys. In order to successfully include the new material into existing processes, investigations were performed to obtain an in-depth understanding of the material's properties<sup>5-8</sup>.

Several studies and experiments have been conducted on specific SMT processes. Some were aimed at optimizing process parameters for printing<sup>9-12</sup> or the reflow heating curve, others were aimed at evaluating joint quality when lead-free paste was used in existing processes<sup>13-18</sup>. It is likely that the quality of solder joints would depend both on materials and processes, and it is not easy to set control variables in order to obtain a desired process. The authors observe that, to date, no comprehensive investigation on materials and assembly processes, or transition issues due to lead contamination, has been published.

The objective here is, to a certain extent, to fill this gap, presenting the results of a comprehensive experimentation aimed at optimizing control parameters of manufacturing and at improving solder-joint quality. Once the most widely used paste was identified and its physical and rheological properties verified, an experiment based on the Taguchi approach was carried out to establish the optimal printing parameters. A practical technique is proposed to set the control variables of a reflow oven, which ensure the desired heating curve inside the oven. Then, using the obtained printing parameters and the developed setting technique, the relationship between solder-joint quality and materials used was investigated. To this end, a full factorial experiment was conducted on the entire soldering process to determine the best combination of paste/board finishes and to evaluate the effect of nitrogen ambient and lead contamination. All the results obtained for the lead-free paste were compared with a control sample consisting in standard tin-lead paste and finishing.

As the physical characteristics of solder paste have a direct impact on the main processes of SMT, tests were performed on tin-lead and lead-free pastes used for process experimentations. The tested solders have spherical particle shape (particle size composition of Type 3 according to IPC norms) and no-clean flux. In particular, the tin-lead paste is Sn63Pb37 with 90.5% metal content, while the lead-free paste is Sn95.5Ag4Cu0.5 with an 89.5% metal content.

**Thermal characteristics.** An important issue for lead-free soldering is the thermal management of reflow, since eutectic SnAgCu has shown a melting point of 220°C compared to 183°C for eutectic SnPb. As a consequence the reflow temperature needs to be raised. Pasty range – the temperature difference between solids and liquids – is close to zero (2°C for SnPb and 1°C for SnAgCu), as both tin-lead and lead-free alloys are eutectic, and so they satisfy the conventional 10°C limit (an excessively large pasty range may negatively affect joint reliability due to potential high internal stresses).

**Rheological properties.** As rheological data can predict, to a certain extent, paste printability when compared with other pastes, we performed a series of tests to evaluate how lead-free paste compares to standard tin-lead. The most important rheological parameter is viscosity that shows how resistive the fluid is to flow, by measuring the force required to move one layer over another. It is expressed by

$$F = \mu A \frac{v}{y} \quad [\text{EQ. 1}]$$

where  $F$  is force,  $\mu$  is coefficient of viscosity,  $A$  is the area of layers,  $v$  is the relative velocity between layers and  $y$  is their distance.

The first test was a single-point viscosity measurement carried out using a standard cone plate viscometer, which ensures that the tested sample experiences uniform shear regardless of the distance from the rotation axis. Viscosity values of 700-800 kCps for tin-lead paste and 570-600kCps for lead-free paste were measured. Even if the difference between the two values is not large, the lead-free alloy clearly shows less viscosity and so it will require different print parameters.

To evaluate the change of viscosity in time, a shelf-life test was run repeating the same viscosity measure after storing the paste for one, seven and 30 days. The results (**Table 1**) show an acceptable performance, even if traditional tin-lead paste behavior is better.

**Table 1:** Shelf-life test results.

	<b>SnPb Paste</b>	<b>Pb-free Paste</b>
After 1 day [kCps]	700	524
After 7 days [kCps]	768	624
After 30 days [kCps]	810	600

Solder paste is a viscous non-Newtonian fluid whose resistance to flow is not constant and which exhibits shear thinning. This is an essential requirement of printing, as paste must flow in and out of stencil apertures during the printing stroke, but must remain in position afterward. Pastes are also thixotropic, and their viscosity does not only depend on the shear rate but also on the shear history of the paste. To evaluate this characteristic a second viscosity test was done using an apparatus with two parallel plates where the shear rate was shifted from a minimum to a maximum and vice versa obtaining a "rheogram" plot of the shear stress ( $\tau$ ) and viscosity ( $\mu$ ) against shear rate, measured continuously (**Figures 1 and 2**).

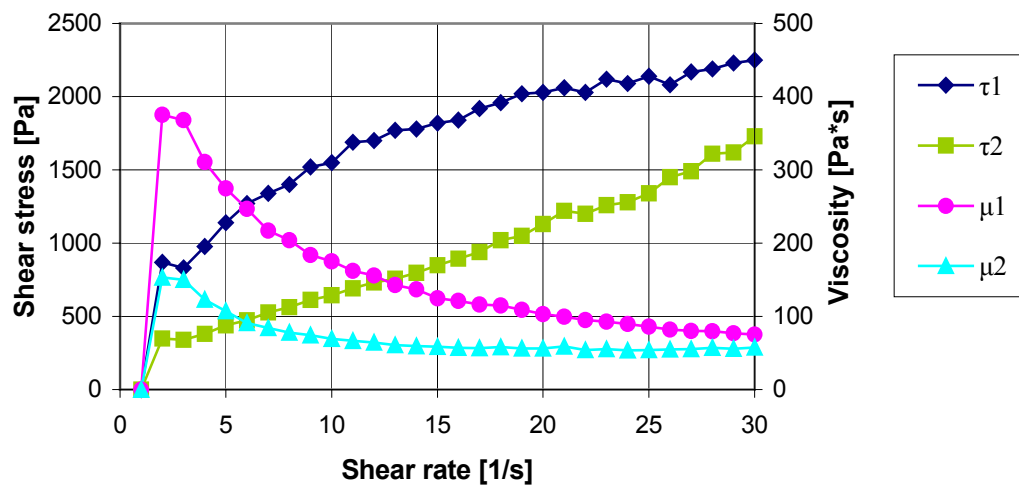


**FIGURE 1:** Rheogram for tin-lead paste.

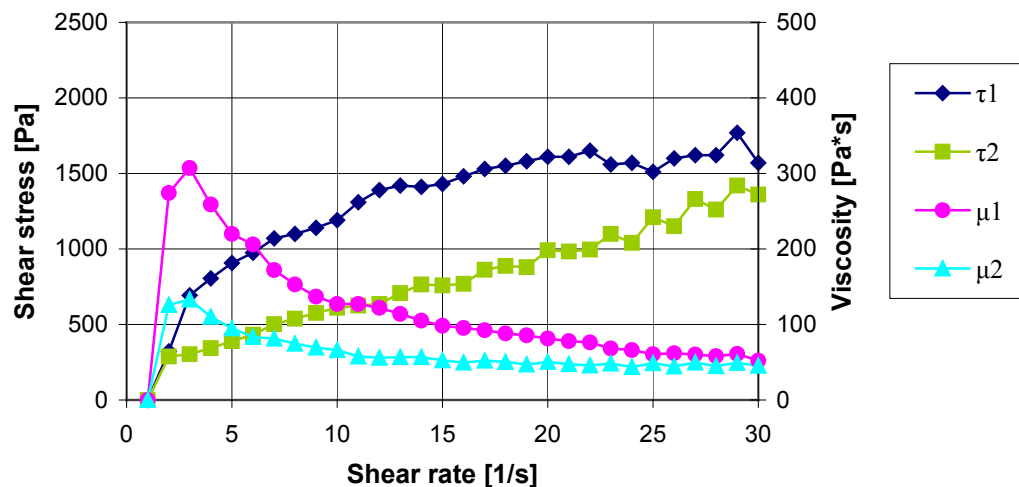


**FIGURE 2:** Rheogram for lead-free paste.

Thixotropic hysteresis may be quantified using a dynamic viscosity index (DVI) defined as follows

$$DVI = \frac{1}{N} \sum_n (\eta_{\max\_n} - \eta_{\min\_n}) \quad [\text{EQ. 2}]$$

where  $\eta_{\max\_n}$  and  $\eta_{\min\_n}$  are the viscosity values at the shear rate  $n$  for increasing and decreasing variations, ranging from  $n = 10^{-1}$  to  $20^{-1}$ . The two values obtained are 72.5 for tin-lead paste and 49.1 for lead-free paste, thus showing a better behavior of the latter.

**Other tests.** A series of additional tests were carried out per IPC-TM-650 to assess other important properties. Wetting balance was performed to determine the ability of the solder paste to wet a copper surface. The solder balls test was carried out to evaluate the propensity of the paste to form solder balls that, if not removed, can create reliability problems by shorting adjacent conductors. Moreover, the tack time test was conducted to determine the ability of a printed pattern of paste to retain a probe placed in the solder by measuring the force required to separate the probe from the paste (this is a measure of how well the paste can keep components in place once positioned by the assembly machine but not yet reflowed). Finally, the slump test was performed to quantify the slump phenomenon. In fact, once the paste is printed, the force of gravity and surface tension work against it, causing the pattern to collapse and spread out from its original boundaries. The test determines a vertical and a horizontal slump for the solder paste.

The test results, summarized in **Tables 2** and **3** and in **Figures 3, 4** and **5**, show that lead-free paste characteristics compare well with those of the standard tin-lead paste even if in some cases (as in the slump test), they are barely acceptable.

**Table 2:** Test Results

Test Type	SnPb Solder Paste	Pb-free Solder Paste
Wetting balance	> 2.2 mN	> 2.2 mN
Solder balls	OK	OK
Tack time (min/max values on 8 hr time)	3.0-4.4 g/mm <sup>2</sup>	2.9-4.3 g/mm <sup>2</sup>

**Table 3:** Slump test results.

Stencil IPC-A-21 (0.20 mm thick)	Pad size: 2.03 x 0.63mm			Pad size: 0.33 x 2.03 mm		
	Acceptable results	Results for tin-lead paste	Results for lead-free paste	Acceptable results	Results for tin-lead paste	Results for lead-free paste
<b>Test 1 (room temperature)</b>	No bridging for spacing >0.56 mm	No bridging	No bridging	No bridging for spacing >0.25 mm	No bridging for spacing >0.10 mm	No bridging for spacing >0.10 mm
<b>Test 2 (150°C)</b>	No bridging for spacing >0.30 mm	No bridging for spacing >0.41 mm	No bridging for spacing >0.63 mm	No bridging for spacing >0.30 mm	No bridging for spacing >0.20mm	Bridging for spacing <0.35 mm

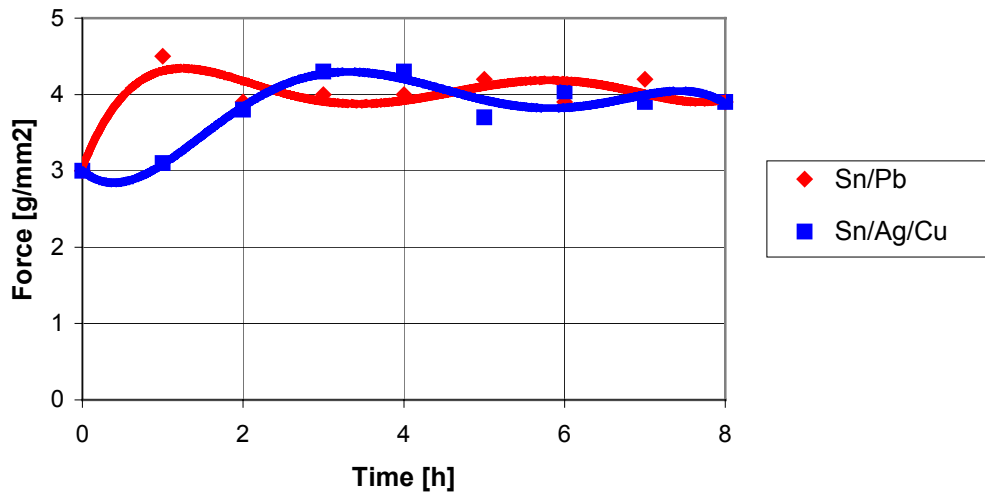


**FIGURE 3:** Tack test.

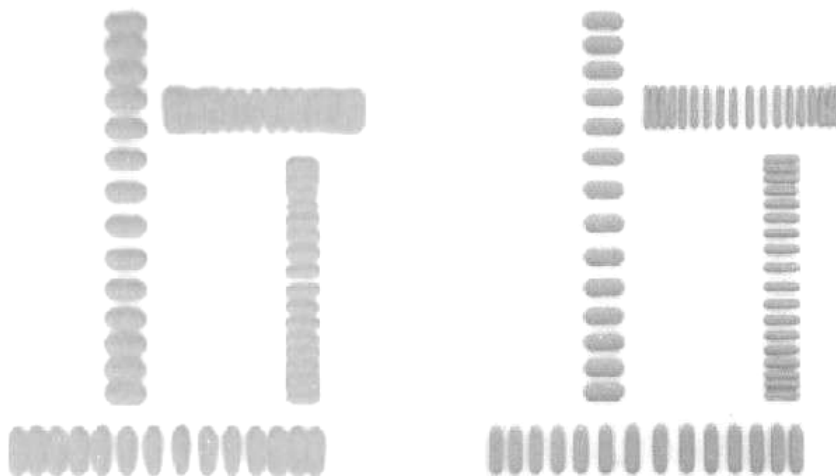


**FIGURE 4:** Sample printed with stencil IPC-A-20.

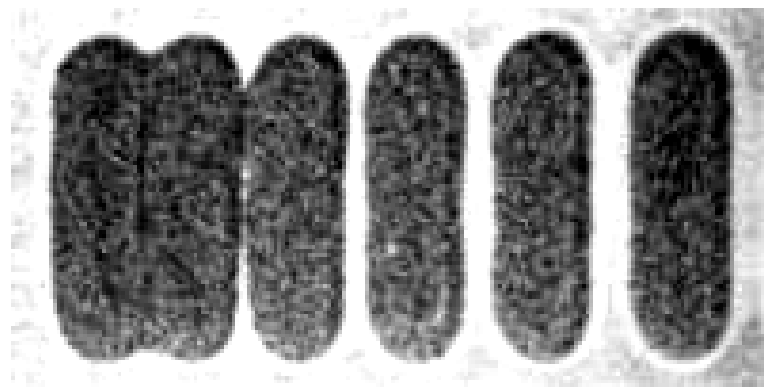


**FIGURE 5:** Slump test.

## Optimal Process Settings

The aforementioned characterization techniques are useful for obtaining information about the pastes regardless of manufacturing process parameters, but do not provide enough data to describe the pastes in terms of printing behavior or reliably predict the effect of reflow. Therefore, we designed tests aimed at optimizing the setting parameters of the critical processes in assembly – printing and reflow – and compared the results of lead and lead-free pastes.

**Paste printing.** Many variables influence the quality of stencil printing, measured by the amount and position of paste deposited. Among them: stencil geometries, paste characteristics, printer settings and quality, substrate and squeegee characteristics. Here, we focus on finding the best printer settings, all other variables remaining fixed. In particular, we selected as variables to be optimized the squeegee speed (the rate the squeegee moves across the stencil), squeegee pressure (the vertical force applied to the squeegee during the print stroke), and the separation speed (the rate at which the board is pulled from the stencil once the print stroke is complete). All remaining process variables were determined based on the engineer's knowledge and experience. The printer was a DEK Horizon model H0Z01 series 278988, the 30 cm squeegees had 60° trailing edge and the snap-off distance was on-contact. We used a 150  $\mu\text{m}$  thick, laser cut, stainless-steel stencil with rectangular apertures with pitches ranging from 120 to 300  $\mu\text{m}$  and apertures for 0.5 mm pitch  $\mu\text{BGAs}$ , 0.8 mm and 1 mm pitch BGAs, 0.5 mm pitch CSPs, QFPs, and 1206, 0805, 0603, and 0402 passives.

For each of the three selected variables (squeeze speed, squeeze pressure and separation speed), we chose three values, also called levels in Taguchi's method. Therefore, in the case of a complete factorial experiment, in which all variable combinations are tested, we would need to perform 27 different tests, while using Taguchi's method we can perform only a limited number of tests, saving money and time. We used the  $L_9(3^4)$  orthogonal Taguchi array, customized for the experiment (**Table**

4) for lead-free and tin-lead pastes. It has nine rows, each corresponding to an experimental test, and three columns, each corresponding to a variable setting. We repeated the nine tests described four times each, in order to minimize the effect of the noise measurement.

**Table 4:** Design of experiments for printing process.

Test	SnPb Paste			Pb-Free Paste		
	Separation speed (mm/s)	Squeeze pressure (kg/cm <sup>2</sup> )	Squeeze speed (mm/s)	Separation speed (mm/s)	Squeeze pressure (kg/cm <sup>2</sup> )	Squeeze speed (mm/s)
1	0.5	6	20	0.7	6	20
2	0.5	10	60	0.7	8	60
3	0.5	14	100	0.7	10	100
4	1.2	6	60	1	6	60
5	1.2	10	100	1	8	100
6	1.2	14	20	1	10	20
7	2.0	6	100	1.5	6	100
8	2.0	10	20	1.5	8	20
9	2.0	14	60	1.5	10	60

The response variable is the percentage of aperture area filled with paste and it was measured using optical magnifiers. Experiments showed that apertures with pitches of 220 to 300  $\mu\text{m}$  were always fully covered by the paste and were thus excluded from the analysis. Results for each test and for each repetition are shown in **Table 5** with the mean value registered for each test and the signal to noise ratio (S/N) calculated with reference to "higher is the best" quality characteristic, that is

$$MSD = \frac{1}{4} \sum_{i=1}^4 \frac{1}{Y_i^2} \quad S/N = -10 \text{Log}_{10}(MSD) \quad [\text{EQ. 3}]$$

where  $Y_i$  is the result of the repetition  $i$ . Higher S/N ratio is desired as it means that the signal is much higher than uncontrollable noise factors such as temperature, humidity, consistency in measurement of data and so on. From the rough data and following the Taguchi method, we prepared the S/N ratio level total table (**Table 6**), which gives the total response values for each control factor and each level, highlighting in bold the setting for obtaining the best response. The best settings for the tin-lead paste are 20 mm/s (low level) for squeeze speed, 10 Kg/cm<sup>2</sup> (medium level) for squeeze pressure and 1.2 mm/s (medium level) for separation speed. The best settings for the lead-free paste are 60 mm/s (medium level) for squeeze speed, 8 Kg/cm<sup>2</sup> (medium level) for squeeze pressure and 1.5 mm/s (high level) for separation speed. From these results, we conclude that squeegee pressure and separation speed do not significantly change in the transition from tin-lead to lead-free paste, while squeegee speed significantly increases, mainly due to the lower value of the viscosity.

**Table 5:** Results of experiment on printing process.

Test	Tin-lead solder paste						Lead-free solder paste					
	Coverage area [%]				Result	S/N	Coverage area [%]				Result	S/N
	Rep. 1	Rep. 2	Rep. 3	Rep. 4	Mean		Rep. 1	Rep. 2	Rep. 3	Rep. 4	Mean	
1	93.1	91.5	92.3	94.2	92.7	-0.66	76.6	78.2	56.9	75.6	71.8	-3.10
2	88.2	85.0	94.0	80.9	87.0	-1.25	84.3	68.2	69.3	67.2	72.3	-2.93
3	88.4	74.5	84.3	74.8	80.5	-1.96	61.6	69.0	56.8	64.0	62.9	-4.10
4	93.3	86.0	93.5	89.2	90.5	-0.88	81.0	80.3	80.2	73.6	78.8	-2.09
5	94.6	86.9	94.0	79.2	88.7	-1.11	79.8	82.6	69.8	69.6	75.5	-2.52
6	97.6	92.8	95.3	95.0	95.2	-0.43	81.2	77.6	35.4	70.8	66.3	-5.17
7	52.4	67.9	63.8	79.9	66.0	-3.91	70.4	81.6	71.8	76.4	75.0	-2.54
8	92.1	93.0	96.9	95.8	94.5	-0.50	85.2	81.6	75.2	72.4	78.6	-2.15
9	82.2	93.5	92.7	88.4	89.2	-1.03	80.6	74.2	62.6	78.4	74.0	-2.75

**Table 6:** Level total table for the S/N ratio of paste printing.

	Tin-lead solder paste			Lead-free solder paste		
	Separation speed	Squeeze pressure	Squeeze speed	Separation speed	Squeeze pressure	Squeeze speed
Total of low level	-3.86	-5.45	<b>-1.59</b>	-10.13	-7.73	-10.42
Total of medium level	<b>-2.43</b>	<b>-2.86</b>	-3.16	-9.79	<b>-7.60</b>	<b>-7.77</b>
Total of high level	-5.43	-3.42	-6.98	<b>-7.43</b>	-12.02	-9.16

**Reflow soldering.** Solder paste vendors provide temperature profiles of the board in the oven to be met in order to obtain the best soldering performances. However, ovens do not set the temperature of the boards being processed, but rather the temperature of the heating panels. So, obtaining the desired temperature profile on boards will depend on the proper setting of the panel temperatures.

Here, we describe a technique for setting panel temperatures, which we applied to a specific oven (Conceptronic HVN102 seven-panel convection oven) and to a specific board (benchmark board with thermocouples mounted on it) but is generally valid. The technique consists of three phases: modeling the thermal process inside the oven by means of an approximate analytical model; performing some tests on the specific oven and specific board in order to extract the parameters of the analytical model; using the analytical model with the extracted parameters to determine the oven settings.

First, we model the thermal process inside an oven kept at constant temperature ( $T_F$ ) by an exponential law

$$T(t) = T_0 e^{-t/\tau} + T_F (1 - e^{-t/\tau}) \quad [\text{EQ. 4}]$$

where  $t$  denotes the time,  $T$  is the temperature measured on the board inside the oven,  $T_0$  is the initial temperature of the board and  $\tau$  is a time constant, which depends on the oven and on the board.

Then, we determine the value of the time constant  $\tau$ , setting all of the oven panels to a constant temperature ( $T_F$ ) and recording the time-temperature diagram of the board, as shown in **Figure 7**.

As there are some time intervals during which the temperature remains constant (when the board passes between two adjacent panels), we eliminated these intervals from the time-temperature diagram and matched the resulting diagram with the analytically one obtained using the exponential law. From the matching, we extracted the time constant  $\tau$ . In particular, we extracted  $\tau_1 = 22.27s$ , setting the oven temperature at  $T_F = 90^\circ C$ , we extracted  $\tau_2 = 25.12s$  setting  $T_F = 160^\circ C$ , and  $\tau_3 = 25.97s$  setting  $T_F = 230^\circ C$ . The dependence of the time constant on the oven temperature clearly shows that the exponential law is not exactly correct, but the averaged value of the time constants is accurate enough for our purposes ( $\tau = 24.5s$ ).

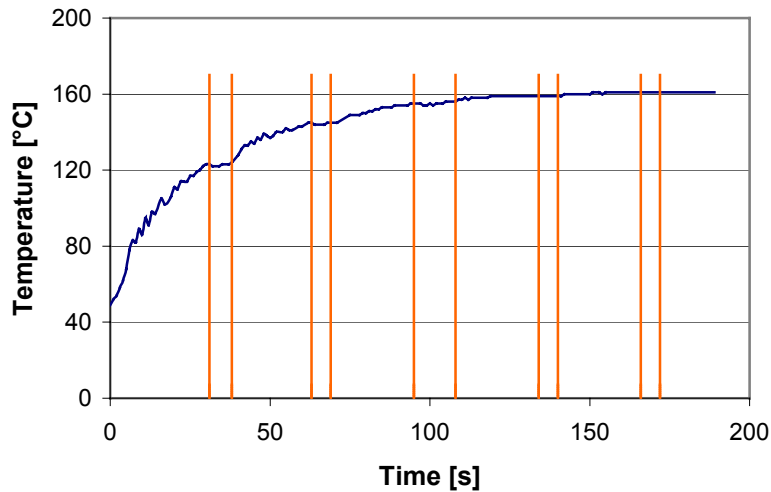


**FIGURE 7:** Temperature recorded on test-board inside an oven at constant temperature.

Finally, we determine the oven control parameters that ensure the desired temperature profile on the board. The conveyor speed ( $v_c$ ) is set as the ratio between the oven length ( $L_o$ ) and the time that the board should stay inside the oven ( $\bar{t}$ ), that is  $v_c = L_o/\bar{t} = 264cm/4min \cong 70cm/min$ . Knowing the conveyor speed and the length of the oven zones, the instants when the board crosses the ending edge of the panels are calculated and reported in **Table 7**.

**Table 7:** Calculated parameters and panel temperature settings for the reflow oven (\* increased by 4%).

Oven panels	Position of the ending edge of the panel [cm]	Crossing instant of the ending edge [s]	$T_S$ [°C] (from the desired profile)	$T_E$ [°C] (from the desired profile)	$T_P$ [°C] (calculated)
1	30	25	30	85	116
2	67	56	85	115	132
3	105	88	115	145	162
4	142	118	145	160	168
5	188	156	160	185	199
6	226	188	185	219	238
7	263	220	219	245	270*

Thus, we calculated the setting temperature of each panel,  $T_P$ , using the exponential law with the extracted time constant  $\tau$

$$T_P = \frac{T_S - T_E e^{-t_C/\tau}}{1 - e^{-t_C/\tau}} \quad [\text{EQ. 5}]$$

where  $t_C$  is the time required by the board to cross the specific panel,  $T_S$  is the temperature at the start of the panel and  $T_E$  is the desired temperature at the end of the panel, as extracted by the time-temperature profile provided by the solder paste vendor. Anyway, in the final area of the oven there is a strong temperature decrease, leading to significant temperature gradients within the board, which reduces the accuracy of the approximate exponential model. We empirically found that it is sufficient to increase the calculated temperature of the last panel by 4% to improve the accuracy.

The setting values of the temperatures of oven panels are reported in **Table 7**, while the measured temperature profile and estimated one are reported in **Figure 8**, showing a good performance of the proposed oven model and panel-setting procedure.

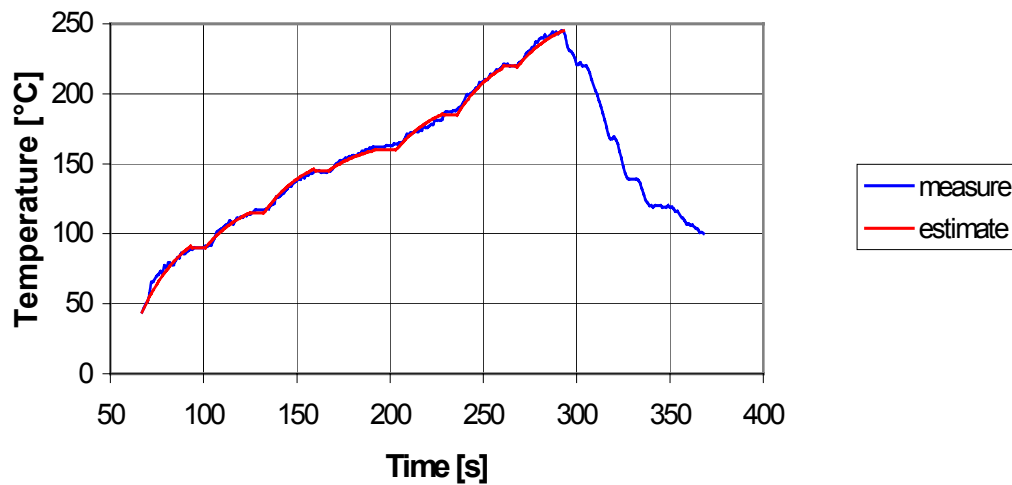
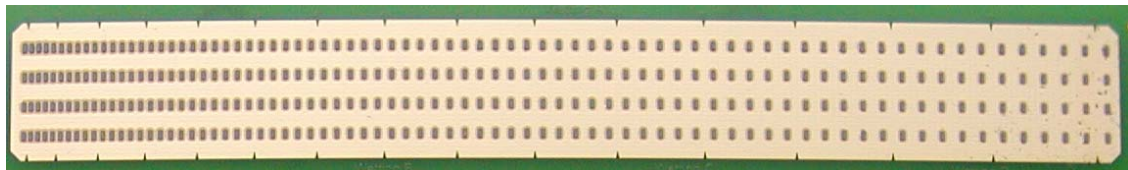


**FIGURE 8:** Measured and estimated temperature profile of the test-board.

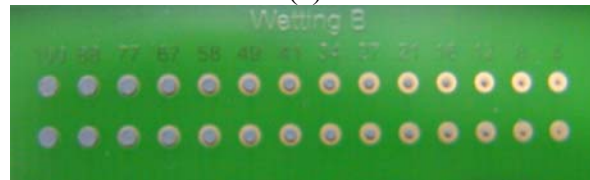
## Joint Quality Evaluations

An experiment on the entire soldering process was performed in order to evaluate the quality of the joints. It was conducted using a test coupon produced by Heraeus (Benchmarker II) to highlight the mechanical characteristics of the joints as well as wettability and solder ball formation. The process parameters used in the experiment are those obtained in the previous section as the best settings.

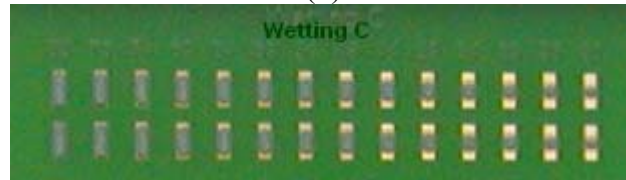
**Wettability and solder balls.** The test coupon has four areas that are used to evaluate the global wetting index (*WIG*) of the solder paste. In the first area, called wetting area A (**Figure 9a**), solder paste is printed with pitches varying from 0.010" to 0.085", and wettability is measured by the number of bridges after reflow (*WIA*). The other three areas, wetting area B, C and D (**Figures 9 b, 9c and 9d**), have 14 pairs of pads, circular or rectangular in shape. Paste is printed starting from a 1:1 ratio and then on smaller and smaller areas of the pads, and wettability is measured by identifying the number of pads fully covered by paste after reflow (*WIB*, *WIC*, *WID*). The global wetting index (*WIG*) is a weighted mean  $WIG = 0.3WIA + 0.3WIB + 0.2WIC + 0.2WID$ , assuming values in the range 0-14.



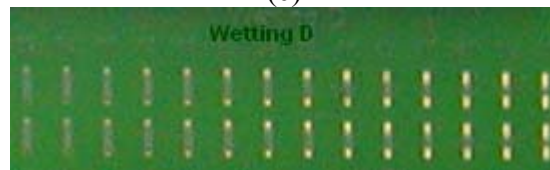
(a)



(b)



(c)



(d)

**FIGURE 9:** Board for wettability test:  
a) wetting area A; b) wetting area B;  
c) wetting area C; d) wetting area D.

The test coupon has also some areas that are used to evaluate solder balls produced during reflow. The area shown in **Figure 10** has a circular zone of 0.8 cm diameter without metal, on which the paste is printed, with a small metal pad in the center. During reflow, the melting alloy is attracted by the central pad leaving the area without metal free and, at the end of process, this zone is analyzed by means of a 20x magnifier in order to find possible solder balls.

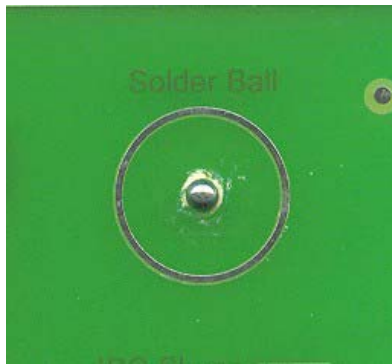


**FIGURE 10:** Solder balls area on the test board.

As process variables, we considered board finishes and reflow ambient, and kept the temperature constant during the experiment. The results obtained for solder balls were very good both for tin-lead and lead-free finishes. The results for the wettability, **Table 8**, show that traditional tin-lead paste has a higher wettability compared to lead-free paste and that better results are obtained in inert ambient.

**Table 8:** Wetting global index (WIG).

	Tin-lead solder paste		Lead-free solder paste	
	Reflow ambient		Reflow ambient	
	Air	Nitrogen	Air	Nitrogen
<b>Board finishes</b>				
SnPb	5.6	8.8	2.3	5.4
Au	7.4	13.7	8.0	11.5
Cu (Entek)	6.1	10.8	1.5	2.1
Chemical Sn	7.5	9.7	7.4	9.3

**Mechanical characteristics.** Solder joint reliability depends on the solder alloy and the materials used for board and component finishes. In the transition between tin-lead based processes and lead-free processes it is foreseeable that leaded and lead-free materials will be used together. Therefore, in order to investigate their interaction, we considered as process variables the board and component finishes besides the solder paste and the reflow ambient. For component finishes, solder paste and reflow ambient we chose two possible values, while for the board finishes we chose four possible values. Therefore, in order to test all of the possible combinations we need 32 tests, each one repeated 10 times to reduce the noise influence, leading to a total of 320 boards. The combinations of the process variables that were tested and the components, both integrated and discrete, placed on the test boards, are shown in **Table 9**.

**Table 9:** Tested combinations of process variables and components placed on test boards.

Test	Process variables				Chips mounted on the boards				Integrated comp. mounted on the boards		
	Comp. finishes	Solder paste	Board finishes	Reflow ambient	1206	805	603	402	BGA 100	SOIC	BQFP
1	Tin-lead	Tin-lead	SnPb	Air	22	22	97	14	2	2	0
2	Tin-lead	Tin-lead	SnPb	Nitrogen	22	22	97	14	2	2	0
3	Tin-lead	Tin-lead	Au	Air	22	22	97	14	2	2	0
4	Tin-lead	Tin-lead	Au	Nitrogen	22	22	97	14	2	2	0
5	Tin-lead	Tin-lead	Cu (Entek)	Air	22	22	97	14	2	2	0
6	Tin-lead	Tin-lead	Cu (Entek)	Nitrogen	22	22	97	14	2	2	0
7	Tin-lead	Tin-lead	Chemical Sn	Air	22	22	97	14	2	2	0
8	Tin-lead	Tin-lead	Chemical Sn	Nitrogen	22	22	97	14	2	2	0
9	Tin-lead	Lead-free	SnPb	Air	22	22	97	14	2	2	0
10	Tin-lead	Lead-free	SnPb	Nitrogen	22	22	97	14	2	2	0
11	Tin-lead	Lead-free	Au	Air	22	22	97	14	2	2	0
12	Tin-lead	Lead-free	Au	Nitrogen	22	22	97	14	2	2	0
13	Tin-lead	Lead-free	Cu (Entek)	Air	22	22	97	14	2	2	0
14	Tin-lead	Lead-free	Cu (Entek)	Nitrogen	22	22	97	14	2	2	0
15	Tin-lead	Lead-free	Chemical Sn	Air	22	22	97	14	2	2	0
16	Tin-lead	Lead-free	Chemical Sn	Nitrogen	22	22	97	14	2	2	0
17	Lead-free	Tin-lead	SnPb	Air	22	22	97	14	0	2	1
18	Lead-free	Tin-lead	SnPb	Nitrogen	22	22	97	14	0	2	1
19	Lead-free	Tin-lead	Au	Air	22	22	97	14	0	2	1
20	Lead-free	Tin-lead	Au	Nitrogen	22	22	97	14	0	2	1
21	Lead-free	Tin-lead	Cu (Entek)	Air	22	22	97	14	0	2	1
22	Lead-free	Tin-lead	Cu (Entek)	Nitrogen	22	22	97	14	0	2	1
23	Lead-free	Tin-lead	Chemical Sn	Air	22	22	97	14	0	2	1
24	Lead-free	Tin-lead	Chemical Sn	Nitrogen	22	22	97	14	0	2	1
25	Lead-free	Lead-free	SnPb	Air	22	22	97	14	0	2	1
26	Lead-free	Lead-free	SnPb	Nitrogen	22	22	97	14	0	2	1
27	Lead-free	Lead-free	Au	Air	22	22	97	14	0	2	1
28	Lead-free	Lead-free	Au	Nitrogen	22	22	97	14	0	2	1
29	Lead-free	Lead-free	Cu (Entek)	Air	22	22	97	14	0	2	1
30	Lead-free	Lead-free	Cu (Entek)	Nitrogen	22	22	97	14	0	2	1
31	Lead-free	Lead-free	Chemical Sn	Air	22	22	97	14	0	2	1
32	Lead-free	Lead-free	Chemical Sn	Nitrogen	22	22	97	14	0	2	1

Two types of mechanical loading tests were performed on the boards: pull and test. In the pull test, performed on 208-pin BQFPs, three lines of pins of the tested component are cut, leaving just one line of pins. The component is bored in the center and is pulled by means of a hook inserted in the hole, until breaking is reached (**Figure 11**). The pull test was performed on four of the 10 boards used for

each test. The shear test, performed on SOICs and BGAs, consists in applying a shear stress on the face of the component that does not have pins (**Figure 12**). In particular, as BGA components are square, shear stress has been applied into both possible directions. The shear test was performed on three of the 10 boards used for each test.

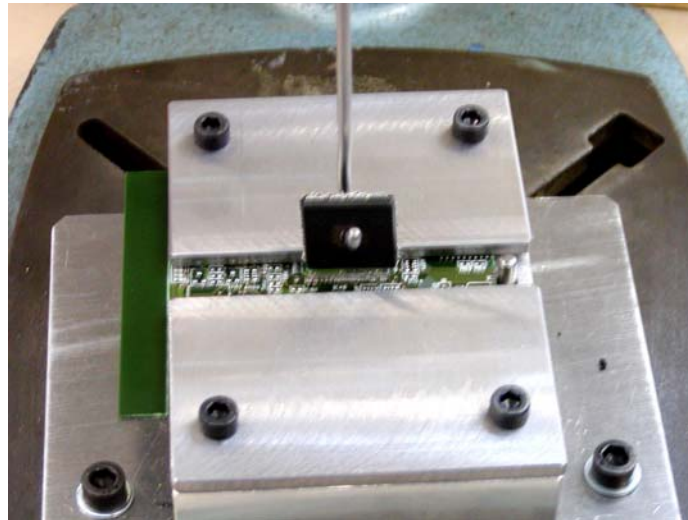


**FIGURE 11:** Pull test.

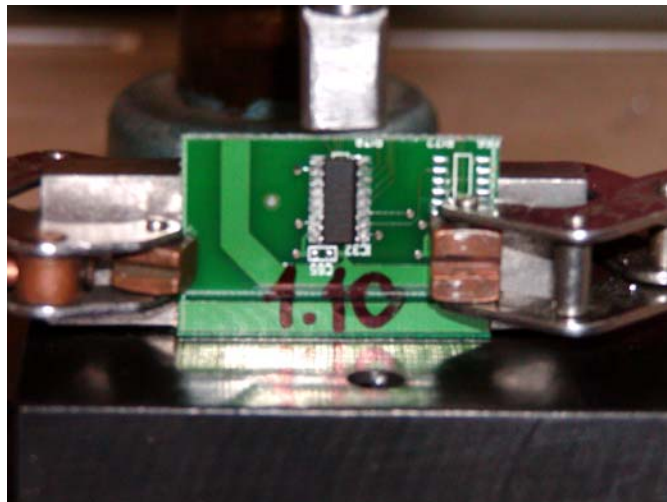


**FIGURE 12:** Shear test.

In almost all the mechanical tests solder joints held out over the breaking values of the pads. Therefore, we can only report in **Table 10** a stress value that is certainly borne by the solder joints.

**Table 10:** Mechanical test results.

Test type	Tested components	Solder joint stress
Shear test	BGA	> 400 g/pin
Shear test	SOIC	>800 g/pin
Pull test	BQFP	>600 g/pin

**Tombstoning effect.** Finally, attention has been devoted to the tombstoning effect, which mainly affects small-size chips<sup>19</sup>. These, as the 0402 and 0201 chips, can lift one terminal changing their position from horizontal to vertical (**Figure 13**). This effect is mainly due to the difference in the stresses applied to the two terminals, which is caused by the difference in the finish wetting for different temperatures at the two terminals of the component, by an excessively strong pre-heat curve, or by a wrong component placement.

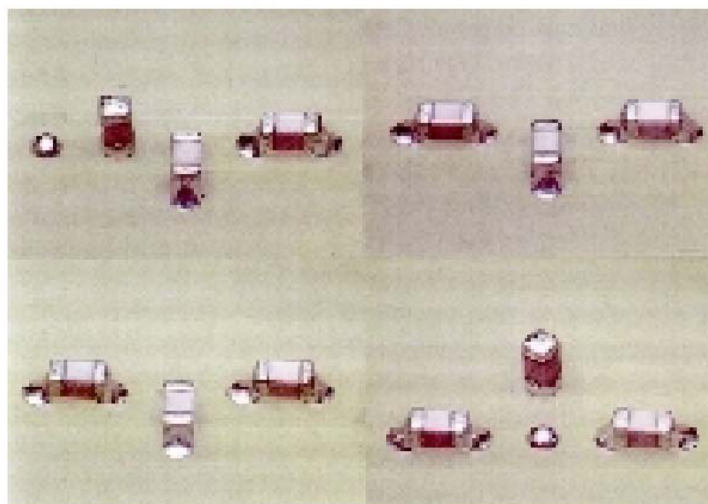


**FIGURE 13:** Tombstoning effect on chips.

The test coupon, Benchmark II board, which is designed to study this effect, presents pads with different geometries that are designed to be covered with different solder paste geometries (**Figure 14, Table 11**). As an example, the pad labeled "H" has a solder coverage area greater than the pad area, while the pad labeled "K" has a solder coverage area reduced with respect to the pad area.

**Table 11:** Pad dimensions for chip 0402.

Label	W [mils]	L [mils]	Z [mils]	Pad geometry	Solder area
A	30	30	14	Rectangle	-10%
B	30	30	16	Rectangle	-10%
C	30	30	18	Rectangle	-10%
D	30	30	20	Rectangle	-10%
E	30	30	22	Rectangle	-10%
F	30	30	24	Rectangle	-10%
G	30	30	26	-10%	
H	30	30	20	Rectangle	+10%
I	30	30	20	Rectangle	0%
J	30	30	20	Rectangle	-10%
K	30	30	20	Rectangle	-10% inside
L	30	30	20	Home plate	-25%
M	30	30	20	Home plate	-33%
N	30	30	20	Home plate	-41%

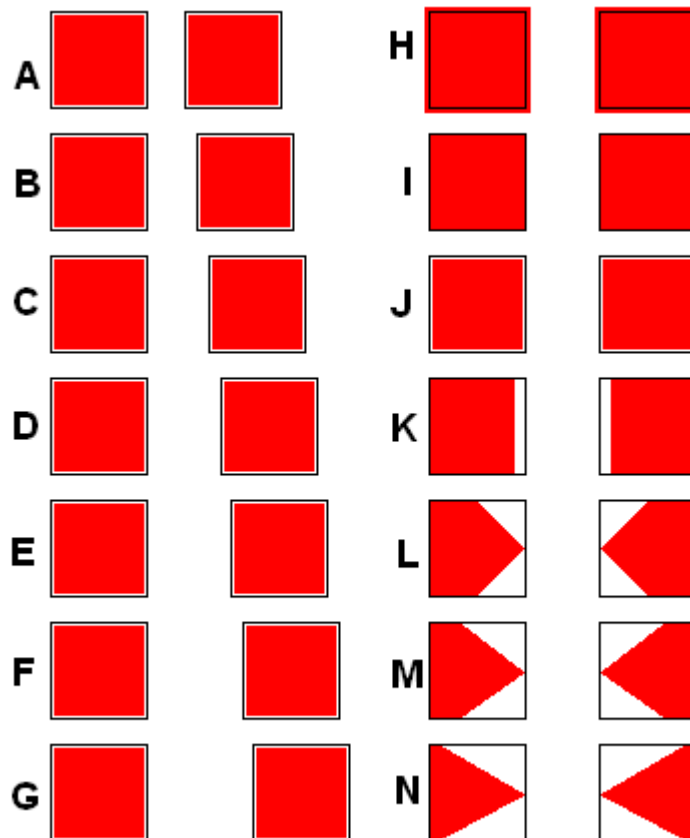


**FIGURE 14:** Pads for 0402 chips.

The results of each of the 32 tests, defined in Table 9, are shown in **Table 12**, and the same results are presented as a function of the pad type in **Table 13**. With reference to pad and solder paste geometries, we observe that the number of tombstones increases with the distance between coupled pads, i.e. Z. Actually, the pads labeled E, F and G showed results far worse than those of type A, B, C, D, I and J. Thus, Z should be less than 0.022". Pad K presented a great number of tombstones, while H showed the best behavior. Finally, the particular form of the deposited paste on pads L, M and N did not ensure good results.

**Table 12:** Results of tests on tombstoning.

<b>Test</b>	<b>1</b>	<b>2</b>	<b>3</b>	<b>4</b>	<b>5</b>	<b>6</b>	<b>7</b>	<b>8</b>	<b>9</b>	<b>10</b>	<b>11</b>	<b>12</b>	<b>13</b>	<b>14</b>	<b>15</b>	<b>16</b>
<b>NT</b>	0	7	0	10	0	9	1	24	2	9	2	7	6	7	9	24
<b>Test</b>	<b>17</b>	<b>18</b>	<b>19</b>	<b>20</b>	<b>21</b>	<b>22</b>	<b>23</b>	<b>24</b>	<b>25</b>	<b>26</b>	<b>27</b>	<b>28</b>	<b>29</b>	<b>30</b>	<b>31</b>	<b>32</b>
<b>NT</b>	2	26	1	46	0	16	0	28	19	25	20	15	22	28	16	31

NT: Number of tombstones obtained in each test.

**Table 13:** Results of tests on tombstoning.

<b>Pad Type</b>	<b>A</b>	<b>B</b>	<b>C</b>	<b>D</b>	<b>E</b>	<b>F</b>	<b>G</b>	<b>H</b>	<b>I</b>	<b>J</b>	<b>K</b>	<b>L</b>	<b>M</b>	<b>N</b>
N.T.	10	8	7	9	24	57	94	4	10	12	88	36	29	24

In order to study the effect of the process variables regardless of pad and solder paste geometries, using Taguchi's method we performed the ANOVA on the results reported in Table 12, obtaining **Table 14**. The higher values of the F statistic obtained for the component finishes and the reflow ambient implies that the tombstoning effect mainly depends on them. Moreover, the level total table for tombstoning effect, reported in **Table 15**, shows that a lower number of tombstones are recorded for tin-lead component finishes and air reflow ambient. The better behavior in air is due to the fact that nitrogen enhances the difference of wettability at the ends of the components, while the better behavior of tin-lead paste is due to the higher surface tension of lead-free paste and the larger temperature differences caused by a more inhomogeneous heating in the case of lead-free solder.

**Table 14:** ANOVA table for tombstoning effect.

	f	SS	MS	F	F_TAB 0,01	S'	%
<b>Component finishes</b>	1	99	99	<b>106</b>	6,63	98	24
<b>Solder paste</b>	1	16	16	17	6,63	15	4
<b>Board finishes</b>	3	16	5	6	3,78	13	3
<b>Ambient</b>	1	140	140	<b>150</b>	6,63	140	35
<b>Interaction comp. vs paste</b>	1	6	6	5,88	6,63		
<b>Interaction comp. vs board</b>	3	15	5	5	3,78	12	3
<b>Interaction comp. vs ambient</b>	1	11	11	11	6,63	10	2
<b>Interaction paste vs board</b>	3	18	6	6	3,78	15	4
<b>Interaction paste vs ambient</b>	1	30	30	32	6,63	29	7
<b>Interaction board vs ambient</b>	3	16	5	6	3,78	14	3
<b>Interaction comp. vs paste vs board</b>	3	11	4	3,76	3,78		
<b>Interaction comp. vs paste vs ambient</b>	1	21	21	22	6,63	20	5
<b>Interaction comp. vs board vs ambient</b>	3	3	1	0,93	3,78		
<b>Interaction comp. vs board vs ambient</b>	3	18	6	6	3,78	15	4
<b>Interaction comp. vs paste vs board vs amb.</b>	3	13	4	4	3,78	10	2
<b>Errors</b>	288	270	1	1		0	3
<b>Total</b>	319	702				402	100

NT: Number of tombstones as a function of the pad type.

**Table 15:** Level total table for tombstoning effect.

	Component finishes		Solder paste		Board finishes		Reflow ambient	
	Levels	N.tomb.	Levels	N.tomb.	Levels	N.tomb.	Levels	N.tomb.
<b>Total, 1<sup>st</sup> level</b>	Tin-lead	117	Tin-lead	170	SnPb	90	Air	100
<b>Total, 2<sup>d</sup> level</b>	Lead-free	295	Lead-free	242	Au	101	Nitrogen	312
<b>Total, 3<sup>d</sup> level</b>	X	X	X	x	Cu (Entek)	88	x	x
<b>Total, 4<sup>th</sup> level</b>	X	X	X	x	Chemical Sn	133	x	x

**Voiding.** X-ray inspection of all BGA components was performed to detect defects of the solder joints. No defects were noted with the tin-lead paste, while some voiding was observed with the lead-free paste. The impact of voids on quality and reliability of solder interconnection has not been investigated in detail yet, although some earlier studies pointed out that reliability increases for joints that contain voids up to a certain size. While large voids surely affect the mechanical and thermal properties of the interconnection and may reduce reliability, a certain level of voiding is generally accepted for BGA joints. Based on experience and IPC guidelines the voids observed are not expected to create

reliability problems; however, this does represent an area of potential concern to be kept under tight control.

Experiments were performed on the main critical steps of SMT process confirming that lead-free soldering based on Sn95.5Ag4Cu0.5 paste is technically viable.

Taguchi analysis of the results determined the best settings of the printing process and a new procedure for determining the optimal setting of a reflow oven. Differences between physical characteristics of the Sn95.5Ag4Cu0.5 paste and the eutectic SnPb paste imply that optimal settings are different. In particular, lead-free optimal printing parameters are a higher squeeze speed and an increased minimum soldering temperature up to 240°C, owing to the lead-free paste's higher melting point.

An experiment on the entire assembly process was performed and analyzed using the Taguchi approach, obtaining results on the dependence of solder joint quality on component and board finishes and on the reflow ambient. In particular, we highlighted the following points:

The higher surface tension of lead-free paste increases the tendency toward tombstoning, which can be kept under control only through correct footprint design.

Nitrogen ambient increases wettability but, in combination with lead-free paste, increases tombstoning significantly. Chemical tin appears to be the board finish, showing the best cost/wettability performance. No evidence of lead contamination affecting joint quality was found in any of the various combination investigated.

X-ray inspection of BGA components soldered using lead-free paste exhibits higher levels of voiding. This phenomenon, even if within IPC limits, needs further investigation to gain better insight into the process parameters that may influence it (i.e., reflow temperature profile, flux type, etc.). This investigation will be subject of further research.

## **Acknowledgments**

The authors would like to acknowledge and thank the many unnamed contributors of IXFIN S.p.A. that made the test program possible. Special thanks to F. d'Ambrosio, G. dello Stritto and R. Gravina for their support during the whole project.

## References

5. M. Arra, D.J. Xie, D. Shangguan, "Performance of Lead-Free Joints Under Dynamic Mechanical Loading," Electronic Components and Technology Conference, 2002.

6. J.R. Ellis, G.Y. Masada, "Dynamic Behavior of SMT Chip Capacitors During Solder Reflow," *IEEE Trans. On Components, Hybrids, and Manufacturing Technology*, vol. 13, no. 3, 1990.

7. R.J. K. Wassink, *Soldering in Electronics*, Electrochemical Publications Ltd., 1989.

**Antonio Buonomo** is professor of electronics at the Dipartimento di Ingegneria dell'Informazione, Seconda Università di Napoli, Naples, Italy. **Alessandro Lo Schiavo** is assistant professor of electronics. **Fabrizio Rotulo** is manager of Ixfin Engineering Division and Campus in Marcianise (Ce) Italy.